• *Invited Research Article*

Metal Oxide Nanostructures from Simple Metal-oxygen Reaction in Air

Ting YU† *and Zexaing SHEN*
Division of Physics and Applied Physics, School of Physical & Mathematical Sciences, Nanyang Technological University, Singapore 637371, Singapore

[Manuscript received December 11, 2007, in revised form February 19, 2008]

Ting YU received his Bachelor degree in Physics from Jilin University (China) and his Ph.D. degree from the National University of Singapore (NUS). In 2003–2005 he was a Postdoctoral Researcher (Singapore Millennium Foundation Postdoctoral Fellowship) at Physics Department of NUS. Since 2005 he has been a faculty member in Physics and Applied Physics Division of Nanyang Technological University (Singapore). Beside his interest in nanoimaging, he also works in the field of controllable fabrication and physical properties of metal oxide nanostructures.

Metal oxide nanostructures (CuO, Co_3O_4, ZnO and α-Fe_2O_3) have been successfully fabricated by a simple and efficient method: heating the appropriate metals in air at low temperatures ranging from 200 to 400°C. The chemical composition, morphology and crystallinity of the nanostructures have been characterized by micro-Raman spectroscopy, X-ray diffraction, scanning electron microscopy and transmission electron microscopy. Two mechanisms: vapor-solid and surface diffusion play dominant roles in the growth of metal oxide nanostructures starting with low melting point metals (Zn and Cu) and high melting point metals (Fe and Co), respectively. With sharp ends and large aspect ratio, the metal oxide nanostructures exhibit impressive field-induced electron emission properties, indicating their potentials as future electron source and displays. The water wettability and anti-wettability properties of iron oxide nanoflakes were also discussed in this work.

KEY WORDS: Metal oxide; Nanostructures; Field emission; Wettability

1. Introduction

Metal oxide nanostructures possessing many attractive properties, such as chemical stability, various electron band configurations and unique magnetic behaviors, have great potential for applications as chemical or biological sensors, electron-field emitters, electrodes of lithium-ion batteries and lasers. These structures have received intensive research interests and become one of the most important members in the nanostructure family[1–7]. Many methods have been developed to fabricate metal oxide nanostructures[8–13]. Among them, vapor-liquid-solid (VLS) and vapor-solid (VS) are most widely used as they are well suited for growth of single crystalline structures with a relatively large scale. However, some disadvantages are also associated with the VLS and VS techniques. For example, an elevated temperature normally ≥1000°C is required to vaporize the metal or metal oxide source. Special care has to be afforded on the atmosphere, flow rate and substrate location. For the VLS process, catalyst introduced to trigger nucleation and initial growth of nanostructures may modify the properties of metal oxide nanostructures and affect the functions of nanodevices[1].

There is on-going interest to find novel methods to synthesize metal oxide nanostructures. In this work, we report a simple and straightforward way to fabricate metal oxide nanostructures by direct reacting metals (foil and film) with oxygen in air at a lower temperature (200–400°C). Our attempts successfully demonstrate that single crystalline metal oxide (CuO, Co_3O_4, ZnO and α-Fe_2O_3) nanostructures on various substrates (metal foil, Si wafer, glass slide, atomic force microscopy (AFM) tip and nanowire) with different morphologies (nanowire, nanowall and nanoflake) could be readily fabricated by this simple method. Considering the melting point of the starting metals and the crystal structure of the nanostructures, the growth mechanisms were attributed to VS (for ZnO and CuO) and surface diffusion (for Co_3O_4

† Ph.D., to whom correspondence should be addressed, E-mail: yuting@ntu.edu.sg.

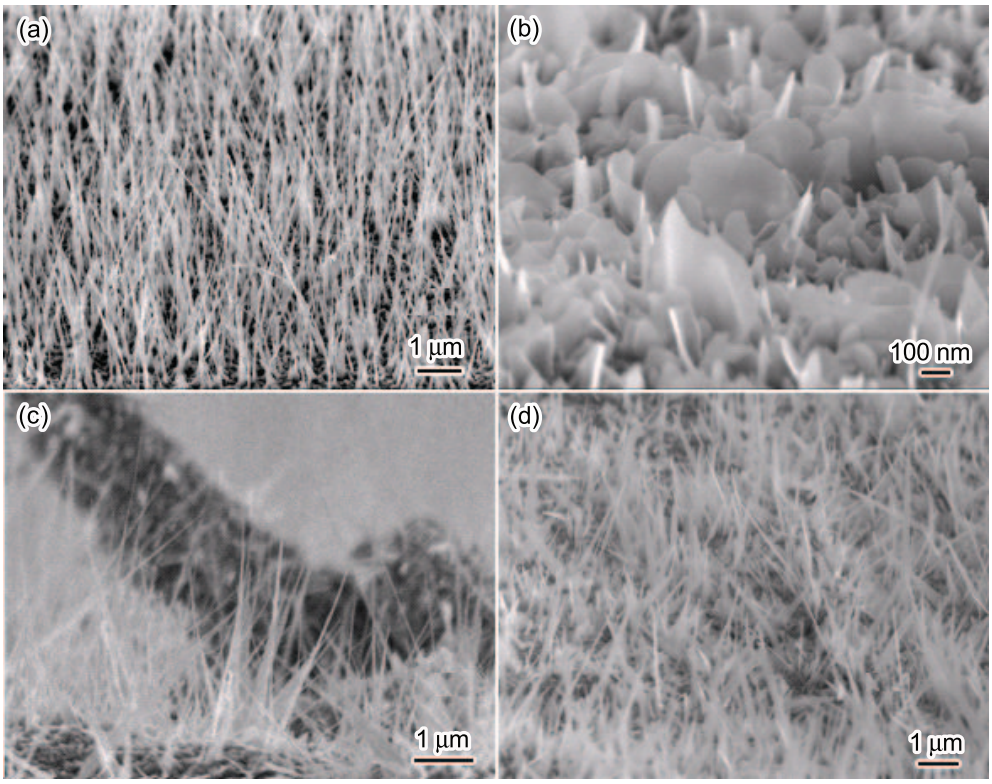

Fig.1 SEM images of the top surfaces of the Cu (a), Co (b), Zn (c) and Fe (d) foil heated at 400, 350, 375 and 260°C for 10 h, respectively

and α-Fe_2O_3), respectively. Considering that the sharp tips or narrow edges of nanostructures can effectively enhance local electric fields and consequently enhance the efficiency of emission, investigations of field-induced electron emission from these metal oxide nanostructures were performed and the results indicate their potentials as high brightness electron source and field emission display media. The wetting behavior of solid surfaces by a liquid is a very important aspect of surface chemistry, which may have a variety of practical applications[14]. Here, water wettability and anti-wettability of iron oxide nanoflakes were also studied. Both hydrphobicity and hydrophilicity were achieved and tuned from one to the other.

2. Experimental

Experimentally, fresh metal foils (Cu, Co, Zn and Fe) with purity of 99.9% (Aldrich) were polished and cleaned before heated on a hot-plate where metal-oxygen reaction occurred. The metal films with thicknesses ranging from 300–900 nm were deposited onto different substrates by radio-frequency magnetron sputtering (Denton vacuum Discovery 18 system). The morphologies of the starting materials and the final products were monitored by scanning electron microscopy (SEM, JEOL JSM-7=6700F) while the chemical composition and crystal structures were analyzed by micro-Raman spectroscopy (Witech CRM200, λ_{laser}=532 nm), X-ray diffraction (XRD, Bruker D8 with Cu$K\alpha$ irradiation) and transmission electron microscopy (TEM, JEOL JEM 2010F, 200 kV). Field emission measurements were conducted in a vacuum chamber at room temperature under a two-parallel-plate configuration. The water wetting behavior was tested by measuring the contact angle (CA) between the water droplet and the substrate surface (FTA 1000 system).

3. Results and Discussion

3.1 Formation and characterization

Figure 1 presents the SEM images of the top surfaces of Cu (a), Co (b), Zn (c) and Fe (d) foils after heating in air at 400, 350, 375 and 260°C for 10 h, respectively. The majority of the nanostructures orient themselves perpendicular to the substrate. One dimensional (1D) wire or needle-like structures appear on the Cu and Zn foils while 2D wall or flake-like structures present on the Co and Fe foils. Careful measurements reveal that the average length of nanowires is in the range of 6–10 μm in length and 100 nm in diameter. The thickness of walls (Fig.1(b)) is around 20 nm and the sharpness of the flakes (Fig.1(d)), defined by the radius of curvature at the tip is around 5 nm.

To further extend the practical attributes of this method, for example substrate-friendly growth, which is desirable for the nanodevices, the appropriate metal was deposited onto the various types of substrates. As an example, Fig.2(a) and (b) show the SEM images of the as-deposited Fe film on silica microspheres and CuO nanowires, respectively. After heating, nanoflakes were successfully grown on the different substrates as shown in Fig.2(c) and (d). Figure 2(e) demonstrates the success of growth of nanoflakes on the AFM tip cantilever by heating the Fe films. The high magnification image (Fig.2(f)) shows that the nanoflakes preferentially grow perpendicularly to the local surface. Similar 1D and 2D nanostructures (Fig.1(a–c)) were also obtained on Cu, Co and Zn films, respectively, with similar dimension but better

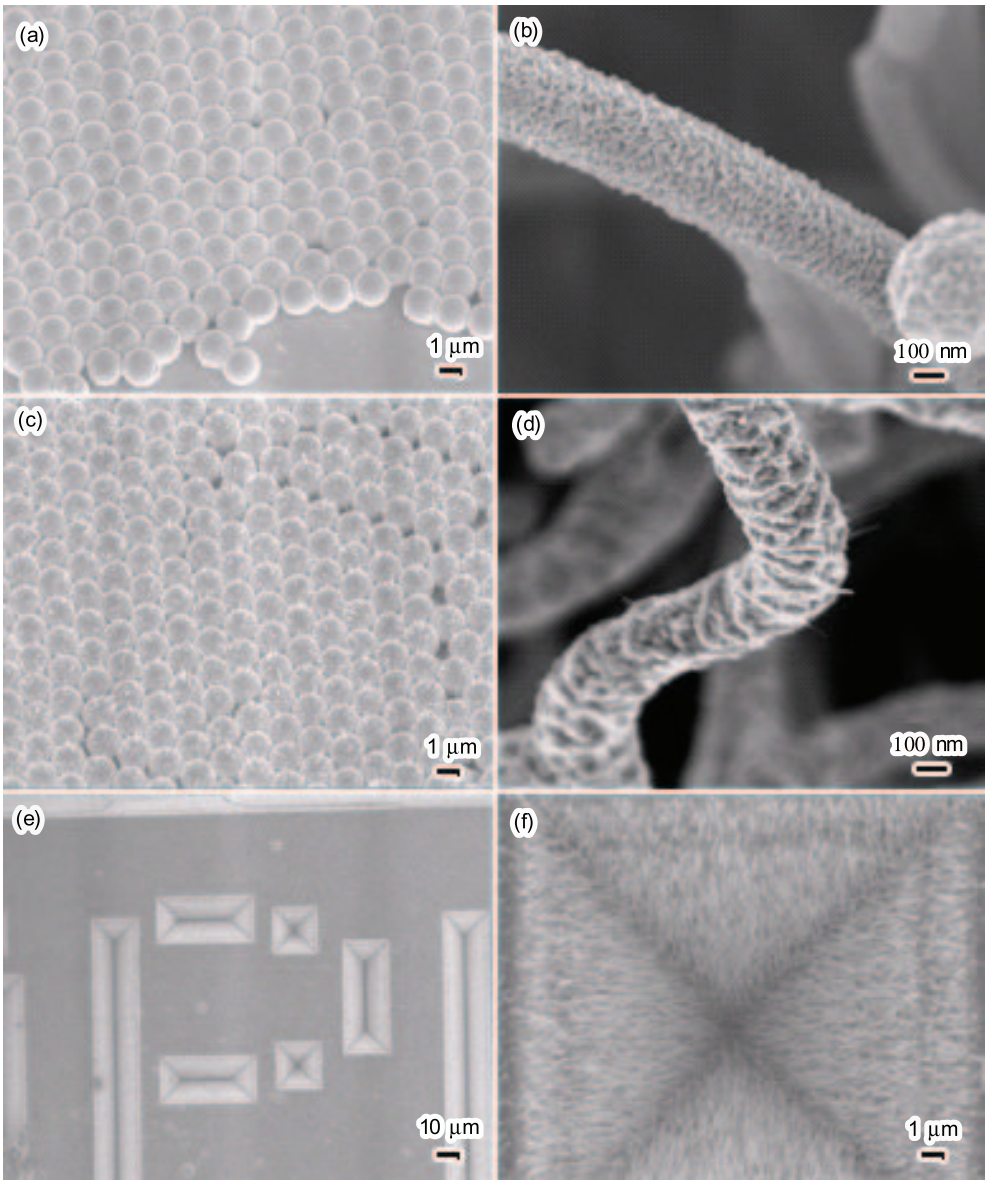

Fig.2 SEM images of the as-deposited Fe films on silica micro-spheres (a) and CuO nanowires (b) and the as-heated samples (c) and (d). (e) and (f) showing the nanoflakes on AFM cantilever

alignment as the surface of films are much flatter than metal foils (SEM images were not shown).

To elucidate the crystal structure and preferential growth direction of the nanostructures, micro-Raman spectroscopy, XRD and TEM were performed. In this paper, Fe oxide was selected to demonstrate the characterization process. Figure 3(a) shows the Raman spectrum of the Fe foil after heating in air. All the peaks could be clearly indexed to crystalline α-Fe_2O_3 or Fe_3O_4 as indicated. The existence of crystalline α-Fe_2O_3 or Fe_3O_4 was also revealed by the XRD of the same sample. The sharp peak located at 45° is the diffraction peak from the Fe foil substrate. It was noted that the most intensive diffraction peak of α-Fe_2O_3 nanoflakes occurred between (110) planes, which differs from bulk α-Fe_2O_3 where the (104) contributes the strongest peak and the ratio between the diffraction peaks from (104) to that from (110) is 1.3[15]. This may imply that there is a preferential growth plane for α-Fe_2O_3 nanoflakes. Figure 3(c) presents typical TEM image of α-Fe_2O_3 nanoflakes. The high-resolution TEM (HRTEM) image was shown in Fig.3(d). The fringe spacing of 0.252 nm matches well with the lattice spacing for the plane (110)[15]. The selected area electron diffraction (SAED) (inset of Fig.3(d)) exhibits a clear diffraction pattern of single crystalline α-Fe_2O_3 from the zone axis of $[\bar{4}41]$. Thus, the XRD and TEM results clearly reveal the growth direction of α-Fe_2O_3 nanoflakes as [110]. The same analysis process confirms the nanostructures shown in Fig.1(a–c) are crystalline CuO, Co_3O_4 and ZnO, respectively[2,9,13].

3.2 Growth mechanism

VLS and VS are two of the most common growth mechanisms. However, from our SEM and TEM images, the VLS process is unlikely in our case because we failed to observe any catalyst terminators on the nanostructures. Similar works[8,16] have demonstrated that VS is responsible for the growth of CuO and ZnO nanowires. Considering that the growth temperatures (250–350°C) are much lower than the melting points of Fe (1353°C) and Co (1495°C)[17], the VS process is likely inexplicable. In our work, we attributed the growth mechanism for Fe and Co to the surface diffusion. At the first stage of heating,

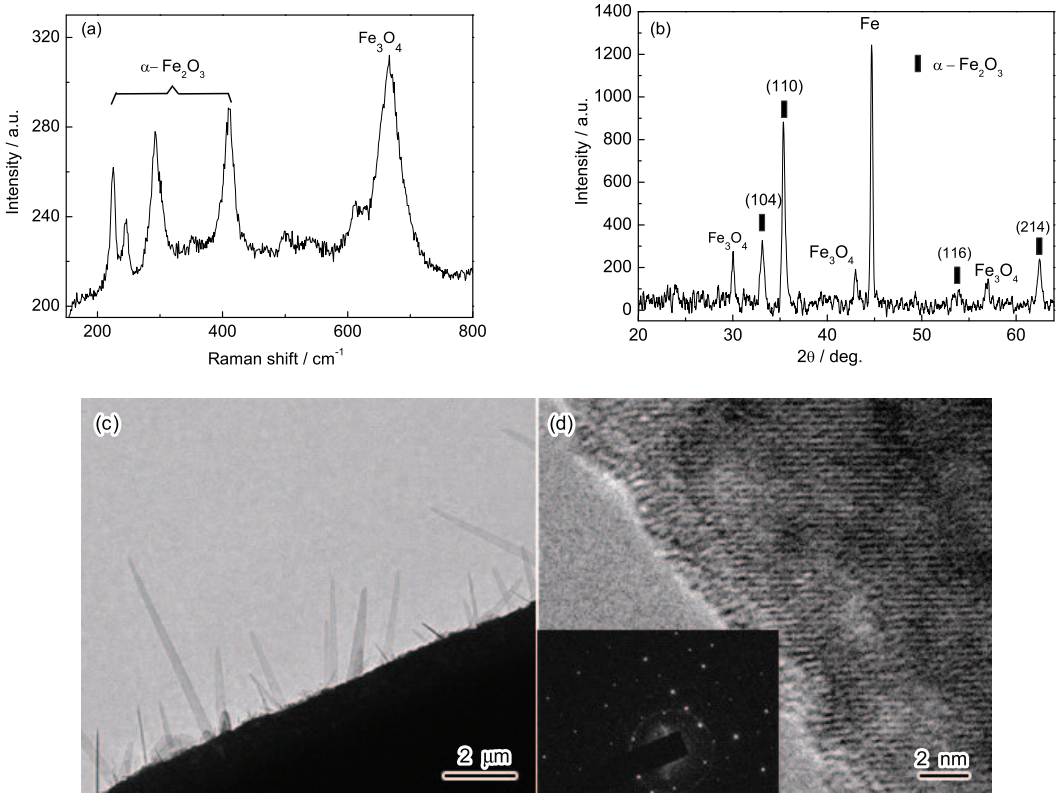

Fig.3 Raman spectrum (a) and XRD pattern (b) of the as-heated Fe oxide sample. The typical TEM and HRTEM images are shown in (c) and (d), respectively. The inset of (d) shows the SAED of α-Fe_2O_3 nanoflake

the top layer of Fe was oxidized by the oxygen molecules in air and formed a very thin layer of α-Fe_2O_3 and Fe_3O_4 mixture. The continuous reaction further oxidized the Fe_3O_4 to α-Fe_2O_3 and formed another layer of Fe_3O_4 below the very top layer of α-Fe_2O_3 by diffusion of oxygen through the thin oxide layer. During the formation and growth of α-Fe_2O_3 top layer, some screw dislocations might be produced along certain crystal direction to release the stress. This may cause the migration of Fe atoms or oxide molecules adsorbed on the surface along this direction and stack in the corresponding plane to maintain a flake shape. For the growth of α-Fe_2O_3 nanoflakes, the driving force is the O-rich and Fe-deficient property in the (110) plane or along [110] direction, which is the growth direction as revealed by our XRD and TEM results[18].

3.3 Electron field emission and water wetting behavior

We have studied the field emission properties of our metal oxide nanostructures. Here, we use α-Fe_2O_3 nanoflakes as an example. Figure 4(a) shows the typical current density-electric field (I-V) curve. The exponential dependence between the emission current and the applied field, plotted in $\ln(J/E^2)$ *vs* $1/E$ relationship (Fig.4(b)), indicates that the field emission from α-Fe_2O_3 nanoflakes film follows the Fowler-Nordheim (F-N) relationship[19]. The dots are experimental data and the solid line is the fitting curve according to the simplified Fowler-Nordheim equation:

$$J = \frac{A(\beta E)^2}{\phi}\exp\Big[-\frac{B\phi^{\frac{3}{2}}}{\beta E}\Big] \qquad (1)$$

where J is the current density; E is the applied field strength; Φ is the work function for electron emission, which is estimated to be 5.4 eV[20] for α-Fe_2O_3; A and B are constants with the value of 1.54×10^{-6} ($A\cdot V^{-2}\cdot eV$) and 6.83×10^{7} ($V\cdot cm^{-1}\cdot eV^{-3/2}$)[4], respectively. Here, β is the field enhancement factor defined by:

$$E_{\text{local}} = \beta E = \frac{V}{d} \qquad (2)$$

where E_{local} is the local electric field nearby the emitter tip; d is the average spacing between the electrodes (d=100 μm in this work) and V is the applied voltage. For the α-Fe_2O_3 nanoflakes, β was obtained to be 1131 from the linear fitting of the F-N curve and the turn-on field was measured to be about 7.2 V/μm, which is acceptable for the practical application.

ZnO nanowire is a well-known excellent field emission candidate. In this work, we fabricated ZnO nanowires on transparent ITO (indium tin oxide) glass slide and tested its emission properties. As shown in Fig.4(c) and (d), the "milk-white color" ZnO nanowires cover the entire piece of slide, indicating large scale growth; the "Great Wall of China" background can be clearly seen, demonstrating the transparent property; and the bright "NANO"—emission image reveals the high efficiency and uniformity of the emission. These significantly imply the potential of ZnO nanowires grown by this method in future large-scale flat transparent display.

The large surface to volume ratio and significant roughness has attracted growing attention to study the water wetting behavior of nanostructures for both fundamental understanding and practical applica-

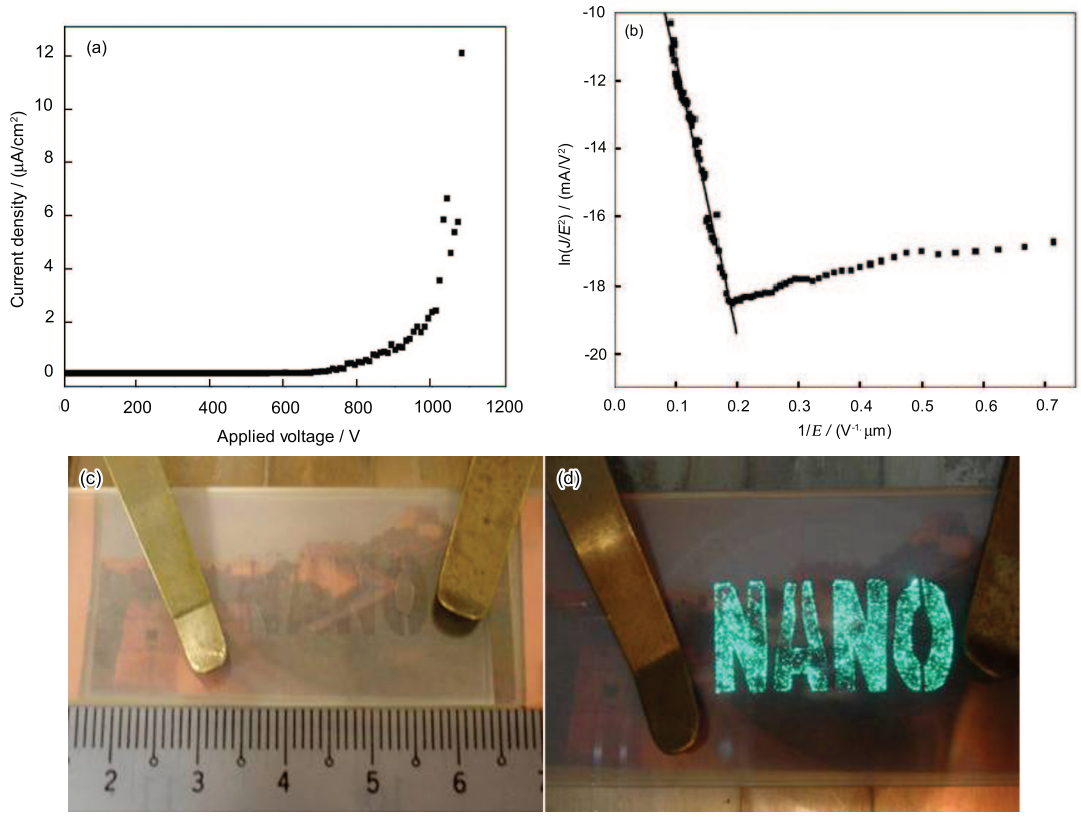

Fig.4 (a) Typical field-emission current-voltage (I-V) curve of the α-Fe_2O_3 nanoflakes films, (b) the F-N plot ($\ln(J/E^2)$ *vs* $1/E$) accordingly, which exhibits a good linear dependence (solid line is the fitting result), (c) optical graph of the as-grown ZnO nanowires on ITO glass slide and (d) electron emission image of the sample shown in (c)

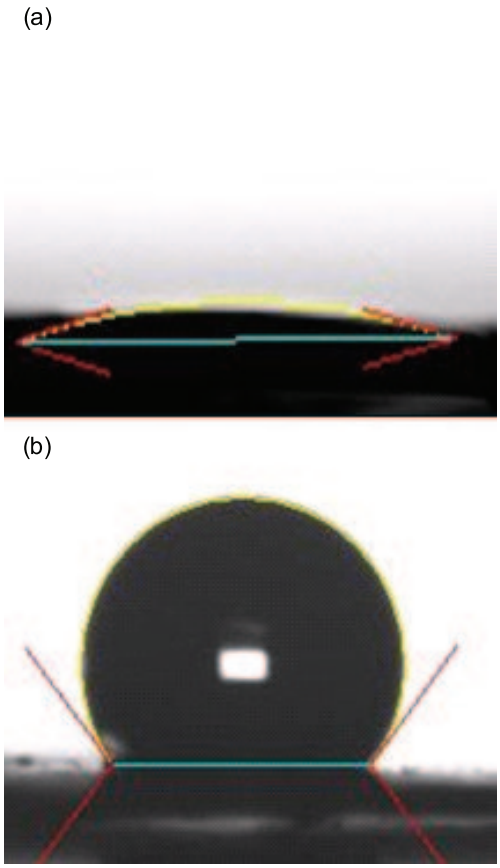

Fig.5 Photographs of water droplet shape on: (a) the as-grown α-Fe_2O_3 nanoflakes, (b) stored in N_2 for 2 d (same piece)

tions. Figure 5(a) shows the optical photograph of water droplet shape on the as-grown α-Fe_2O_3 nanoflakes. The water wettability was evaluated by the water contact angle (CA) measurement. As α-Fe_2O_3 is polar molecule, hydrophilic property of the fresh α-Fe_2O_3 nanoflakes was expected and revealed by a CA of 8° (Fig.5(a)). It is noted that the CA of α-Fe_2O_3 nanoflakes is much smaller than that of α-Fe_2O_3 film (CA=about 30°). This difference could be explained by the dramatic increase of the surface roughness[14]. Interestingly, after stored in a neutral gas environment such as Ar or N_2 for 2 d, the α-Fe_2O_3 nanoflakes changed to be hydrophobic with a CA of 127°. We temporally attributed this to the absorbance of neutral gas molecules, which was supported by transforming the hydrophobicity back to hydrophilicity after heating the α-Fe_2O_3 nanoflakes on a hot-plate again, where desorption of the neutral gas molecules is likely to happen. The detailed study is undergoing in our group. This controllable transformation between hydrophobicity and hydrophilicity might open a new category of potential applications of α-Fe_2O_3 nanoflakes.

4. Conclusion

Single crystalline metal oxide nanostructures have been successfully fabricated by simple reaction between metals and oxygen at low temperatures using hot plates. The practical desirable attributes such as low cost, large scale, substrate-friendly and diversified samples demonstrate that our technique could

be an effective method to supply nanomaterials for further fundamental studies and practical applications. The impressive electron field emission properties from these metal oxide nanostructures indicate their promising potential as electron source and in electron emission displays. The reversible transformation between hydrophilicity and hydrophobicity suggests a new potential for α-Fe_2O_3 nanoflake applications.

Acknowledgement

T.Yu acknowledges the help from Dr Zhang Jixuan and Prof. Sow Chorng-Haur.

REFERENCES

[1] Y.Xia, P.Yang, Y.Sun, Y.Wu, B.Mayers, B.Gates, Y.Yin, F.Kim and H.Yan: *Adv. Mater.,* 2003, **15,** 353.

[2] T.Yu, Y.W.Zhu, X.J.Xu, Z.X.Shen, P.Chen, C.T.Lim, J.T.L.Thong and C.H.Sow: *Adv. Mater.,* 2005, **17,** 1595.

[3] Q.H.Lu, K.L.Yao, D.Xi, Z.L.Liu, X.P.Luo and Q.Ning: *J. Mater. Sci. Technol.,* 2007, **23,** 189.

[4] Y.W.Zhu, T.Yu, C.H.Sow, Y.J.Liu, A.T.S.Wee, X.J.Xu, C.T.Lim and J.T.L.Thong: *Appl. Phys. Lett.,* 2005, **87,** 231031.

[5] M.V.Reddy, T.Yu, C.H.Sow, Z.X.Shen, C.T.Lim, G.V.Subba Rao and B.V.R.Chowdari: *Adv. Funct. Mater.,* 2007, **17,** 2792.

[6] Y.W.Zhu, A.M.Moo, T.Yu, X.J.Xu, X.Y.Gao, C.T.Lim, Z.X.Shen, C.K.Ong, A.T.S.Wee, J.T.L.Thong and C.H.Sow: *Chem. Phys. Lett.,* 2006, **419,** 458.

[7] Y.W.Zhu, H.I.Elim, Y.L.Foo, T.Yu, Y.J.Liu, W.Ji, J.Y.Lee, Z.X.Shen, A.T.S.Wee, J.T.L.Thong and C.H.Sow: *Adv. Mater.,* 2006, **18,** 587.

[8] X.S.Fang and L.D.Zhang: *J. Mater. Sci. Technol.,* 2006, **22,** 1.

[9] T.Yu, Y.W.Zhu, X.J.Xu, K.S.Yeong, Z.X.Shen, P.Chen, C.T.Lim, J.T.L.Thong and C.H.Sow: *Small,* 2006, **2,** 80.

[10] D.J.Qiu, P.Yu, Y.T.Jiang and H.Z.Wu: *J. Mater. Sci. Technol.,* 2006, **22,** 541.

[11] T.Yu, X.Zhao, Z.X.Shen, Y.H.Wu and W.H.Su: *J. Cryst. Growth,* 2004, **268,** 590.

[12] Z.W.Liu, C.K.Ong, T.Yu and Z.X.Shen: *Appl. Phys. Lett.,* 2006, **88,** 053110.

[13] Y.W.Zhu, T.Yu, F.C.Cheong, X.J.Xu, C.T.Lim, V.B.C.Tan, J.T.L.Thong and C.H.Sow: *Nanotechnology,* 2005, **16,** 88.

[14] X.J.Feng and L.Jiang: *Adv. Mater.,* 2006, **18,** 3063.

[15] *Join committee on Powder Diffraction Standards (JCPDS),* Card No. 87 1166.

[16] X.C.Jiang, T.Herricks and Y.N.Xia: *Nano Lett.,* 2002, **2,** 1333.

[17] http://webelements.com, 2008-12-10.

[18] X.G.Wen, S.H.Wang, Y.Ding, Z.L.Wang and S.H.Yang: *J. Phys. Chem. B,* 2005, **109,** 215.

[19] R.Fowler and L.W.Nordheim: *Proc. R. Soc. London Ser. A,* 1928, **119,** 173.

[20] V.E.Hendrich and P.A.Cox: *The Surface Science of Metal Oxides,* Cambridge University Press, Cambridge, UK, 1994.